Optica Applicata, Vol. XVI, No. 4, 1986

Variable wavelength interferometry IV. An alternative approach to the fringe-field method*

Maksymilian Pluta

Central Optical Laboratory, ul. Kamionkowska 18, 03-805 Warszawa, Poland.

The variable wavelength interferometry (VAWI), presented previously, depended on the varying wavelength (λ) of monochromatic light and on selection of such particular wavelengths λ_1, λ_2, λ_3, ... for which interference fringes, displaced by an object under study, were coincident or anticoincident with undisplaced (reference) fringes. Now, a relatively long distance d is selected between two pointer lines in the fringe interference field, the zero-order fringe of the empty interference field is adjusted to the coincidence with one pointer line, and the displaced fringes of high orders $m = m_1$, $m_2 = m_1+1$, $m_3 = m_1+2$, ... are successively led to the coincidences with the other pointer line when the wavelength of monochromatic light is varied from $\lambda = \lambda_1$ to λ_2, λ_3, ... The interference order m_1 is referred to as the initial (or introductory) order which should be selected as high as possible (e.g., $m_1 = 10$ or even more). For this reason, this new approach to the fringe-field VAWI method can be classified into high-order interferometric techniques.

1. Introduction

The original variable wavelength interferometry (VAWI), presented in previous papers [1–3], is especially suitable for the study of objects which produce relatively significant optical path differences δ, say, greater than 3λ (λ is the wavelength of light). For δ smaller than 3λ, the VAWI method suffers from some drawbacks and must be modified. The modification is the purpose of this paper, which should be treated as an alternative version of the original fringe-field VAWI techniques for both transmitted [1] and reflected [3] light. This new version will be marked by the acronym VAWI-2.

The VAWI-2 technique also uses monochromatic light with continuously variable wavelenght, but it is based on another form of fringe coincidence. For this operation a gauging graticule consisting of two pointer lines (or other marks) has now been employed. The zero-order fringe of the empty interference field is adjusted so as to coincide with one pointer line, and the high-order fringes displaced by an object under study are consecutively led to coincidences with the other pointer line, when the wavelength of monochromatic light is continuously

* This work has been presented at the VII Czechoslovakian-Polish Optical Conference, Palkovice (Czechoslovakia), September 8–12, 1986.

varied within the visible spectrum. The distance (d) between the pointer lines should be selected as long as possible. If, however, optical path differences δ, to be measured, are several times greater than λ, say, $\delta \geqslant 10\ \lambda$, the distance d must be reduced to zero, and in this case the VAWI–2 technique takes a form of the original VAWI method.

The VAWI–2 technique is especially suitable for measuring very thin objects which produce small optical path differences. This ability will be demonstrated here and illustrated by measuring examples.

2. Principle

Let us assume that a fringe interference field is produced by superposition of two plane wavefronts Σ_1 and Σ_2 (Fig. 1) inclined to each other at the angle ε. The empty interference field, i.e., the interference pattern not perturbed by the

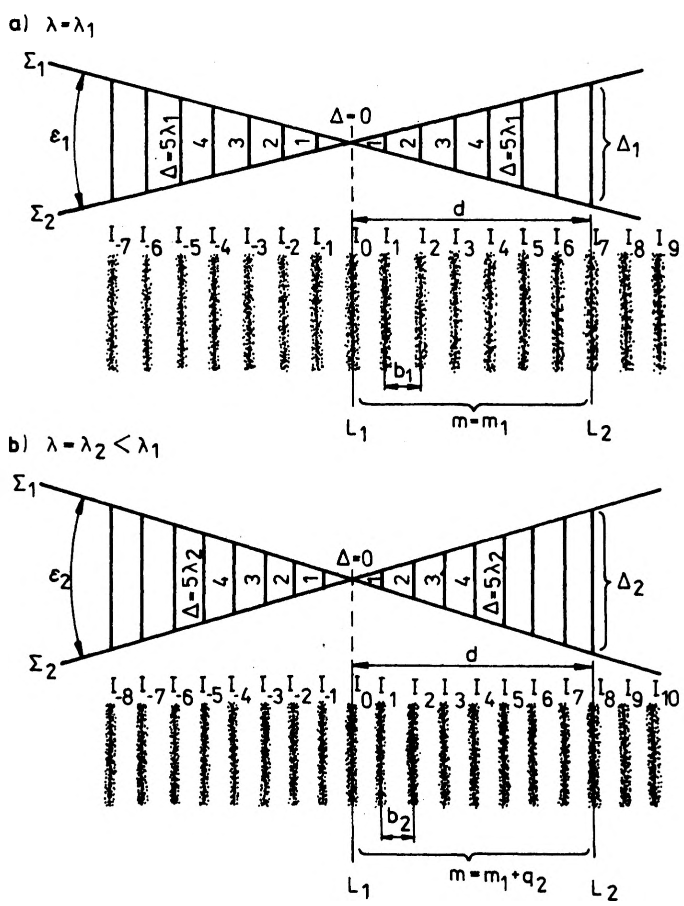

Fig. 1. Principle of VAWI–2 method applied to empty interference field

object under study, is then covered by equally spaced straight-line fringes $\ldots I_{-3}, I_{-2}, I_{-1}, I_0, I_{+1}, I_{+2}, I_{+3}, \ldots$ It is well known that the interfringe spacing b varies with light wavelength λ. The variation manifests itself as the movement of the interference fringes toward the zero-order fringe I_0 when λ becomes shorter and shorter, and, vice versa, the fringes move from I_0 when λ becomes longer and longer. The zero-order fringe occurs along a line where the wavefronts Σ_1 and Σ_2 intersect; here the optical path difference Δ betwen Σ_1 and Σ_2 is equal to zero. The fringes of the first, second, third, and higher orders occur for $\Delta = \pm\lambda, \pm 2\lambda, \pm 3\lambda, \ldots$. These fringes are either bright or dark; the latter are supposed here as produced by polarization interferometers with crossed polars. The zero-order fringe of the empty interference field is readily identifiable in white light as an achromatic one while the others are coloured.

Let us select a distance d measured from the zero-order fringe I_0 to high-order fringes through several interfringe spacings b. This distance is marked by two pointer lines L_1 and L_2. One of these lines L_1 is brought into coincidence with the centre of the zero-order fringe I_0, while the successive high-order fringes are brought into coincidence with the other pointer line L_2, when the wavelength of monochromatic light is varied. The start from the longest red wavelengths permits us to select such a first clearly visible red wavelength λ_1 for which one of the high-order fringes becomes coincident with the pointer line L_2 (Fig. 1**a**). The distance d is now covered by m_1 interfringe spacings b_1, i.e.

$$d = m_1 b_1 \tag{1}$$

where m_1 is referred to as the initial (or introductory) interference order.

From the geometry of Fig. 1**a** it follows that the optical path difference between the wavefronts Σ_1 and Σ_2 at the pointer line L_2 is given by

$$\Delta_1 = 2d \tan\frac{\varepsilon_1}{2}. \tag{2}$$

Usually, the angle ε_1 is very small, thus $\tan(\varepsilon_1/2) \approx \varepsilon_1/2$ and – since $d = m_1 b_1$ and $b_1 = \lambda_1/\varepsilon_1$ – then Eq. (2) can be rewritten as

$$\Delta_1 = d\varepsilon_1 = m_1 \lambda_1. \tag{3}$$

Next, let the wavelength of light be continuously varied from λ_1 to λ_2 for which the pointer line L_2 becomes coincident with a fringe whose interference order is higher by 1 with respect to m_1 (Fig. 1**b**). By analogy with Eq. (3), this coincidence (i.e., the second one) may be expressed as

$$\Delta_2 = d\varepsilon_2 = (m_1 + 1)\lambda_2. \tag{4}$$

Varying the light wavelength through the entire visible spectrum makes it possible to coincide the pointer line L_2 with fringes of integer order higher than $m_1 + 1$. Consequently, Eq. (4) may be rewritten in a more general form

$$\Delta_2 = d\varepsilon_2 = (m_1 + q_2)\lambda_2 \tag{5}$$

where q_2 is a number which expresses the increment of the current interference order m with respect to m_1 when the light wavelength is changed from λ_1 to λ_2, i.e., $m = m_1 + q_2$.

In general, the initial wavelength λ_1 can be selected arbitrarily, and light wavelength can be varied towards both long- and short-wavelength regions of the spectrum. If λ_2 is shorter than λ_1, the increment q_2 is positive ($q_2 > 0$), and, vice versa, this quantity is negative ($q_2 < 0$) when λ_2 is longer than λ_1. Normally, the increment q_2 is selected to be equal to 1, 2, 3, ..., but sometimes it is also useful to select $q_2 = 0.5$, 1.5, 2.5, ... In the latter instance the pointer line L_2 is anticoincident with dark fringes but coincident with bright fringes (Fig. 2). In short, this situation will be called the anticoincidence.

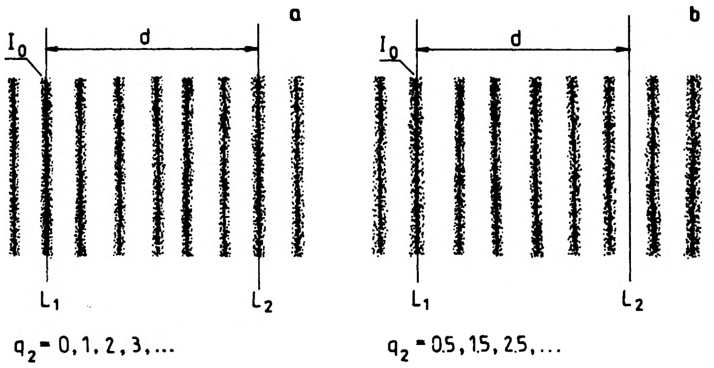

Fig. 2. Coincident (a) and anticoincident (b) positions of interference fringes with respect to pointer line L_2

From Eqs. (3) and (5) it follows that

$$m_1 = q_2 \frac{\lambda_2}{\varepsilon_{21}\lambda_1 - \lambda_2} \tag{6}$$

where

$$\varepsilon_{21} = \frac{\varepsilon_2}{\varepsilon_1}. \tag{7}$$

Here ε_1 refers to the wavelength λ_1 and ε_2 to λ_2. The coefficient ε_{21} expresses the spectral dispersion of the angle between the interfering wavefronts Σ_1 and Σ_2 (see Fig. 1).

Since the interfringe spacing b can be expressed as $b = \lambda/\varepsilon$, Eqs. (3) and (5) may also be written as

$$\Delta_1 = d\varepsilon_1 = m_1 \varepsilon_1 b_1, \tag{8}$$

$$\Delta_2 = d\varepsilon_2 = (m_1 + q_2)\varepsilon_2 b_2. \tag{9}$$

From these equations it follows that

$$m_1 = q_2 \frac{b_2}{b_1 - b_2}. \tag{10}$$

The above formula is more suitable for analysing the empty interference field than that given by Eq. (6).

If the distance d between the pointer lines L_1 and L_2 is sufficiently long, say, $d = 10b_1$, the increment q_2 is several times greater than unity within the visible spectrum, and Eq. (5) or (9) may be developed into several equations with the increments $q_2 = 0.5, 1, 1.5, 2, 2.5, \ldots$. We can therefore write a family of equations as follows:

$$\Delta_1 = d\varepsilon_1 = m_1 \lambda_1 = m_1 \varepsilon_1 b_1, \tag{11a}$$

$$\Delta_2 = d\varepsilon_2 = (m_1 + 0.5)\lambda_2 = (m_1 + 0.5)\varepsilon_2 b_2, \tag{11b}$$

$$\Delta_3 = d\varepsilon_3 = (m_1 + 1)\lambda_3 = (m_1 + 1)\varepsilon_3 b_3, \tag{11c}$$

$$\Delta_4 = d\varepsilon_4 = (m_1 + 1.5)\lambda_4 = (m_1 + 1.5)\varepsilon_4 b_4, \tag{11d}$$

$$\Delta_5 = d\varepsilon_5 = (m_1 + 2)\lambda_5 = (m_1 + 2)\varepsilon_5 b_5, \tag{11e}$$

. . . .

. . . .

These equations express the optical path differences $\Delta_1, \Delta_2, \Delta_3, \ldots$ between the interfering wavefronts Σ_1 and Σ_2 at the pointer line L_2 for the wavelengths $\lambda_1, \lambda_2, \lambda_3, \ldots$. Any combination of two Eqs. (11) gives a formula similar to Eq. (10) from which the initial or current interference order, m_1 or $m = m_1 + q_2$, can be calculated if it cannot be readily identified by visual observation.

Let us now assume that one of the interfering wavefronts, e.g., λ_1 (Fig. 3**a**) traverses a plate-like transparent object of thickness t and refractive index n. The object retards the wavefront phase by $\varphi = 2\pi\delta/\lambda$, where $\delta = (n' - n)t$ and n' is the refractive index of the surrounding medium. The optical path difference between the wavefronts Σ_1 and Σ_2 is now modified, and may be expressed as $\Delta' = \Delta + \delta$, where Δ is that observed in the empty interference field. The modification of the interference field manifests itself as a displacement of fringes $\ldots I'_{-3}, I'_{-2}, I'_{-1}, I'_0, I'_{+1}, I'_{+2}, I'_{+3}, \ldots$ and, in general, the pointer line L_2 is no longer coincident with any interference fringe. However, the coincidence can be restored by varying the light wavelength, and a particular wavelength λ_1 can be selected to produce the initial coincidence as shown in Fig. 3**b**. The interferometric situation at the pointer line L_2 may be expressed as

$$\Delta'_1 = \Delta_1 + \delta_1 = \Delta_1 + t(n'_1 - n_1) = m_1 \lambda_1. \tag{12}$$

It is selfevident that Δ_1 and m_1 are now other than for the empty interference field discussed previously.

If the light wavelength is still varied within the visible spectrum, we can select

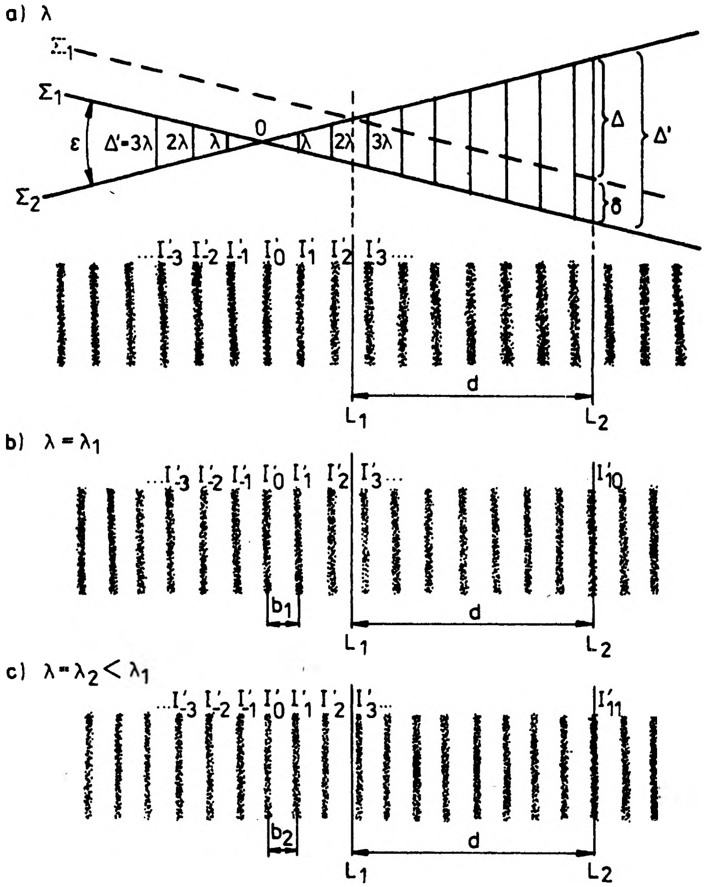

Fig. 3. Principle of VAWI-2 method applied to interference fringes displaced by an object under study

the second particular wavelength λ_2 for which the pointer line L_2 becomes coincident with a fringe whose interference order is equal to m_1+1 (Fig. 3c). By analogy with Eq. (12), this situation at the pointer line L_2 may be described as follows:

$$\Delta'_2 = \Delta_2+\delta_2 = \Delta_2+t(n'_2-n_2) = (m_1+1)\lambda_2. \tag{13}$$

If the distance d between the pointer lines L_1 and L_2 is sufficiently long or δ is much greater than λ, the number of coincidences and/or anticoincidences of the pointer line L_2 with the consecutive interference fringes may be much higher than two. Equation (13) may therefore be rewritten in a more general form

$$\Delta'_2 = \Delta_2+\delta_2 = \Delta_2+t(n'_2-n_2) = (m_1+q_2)\lambda_2. \tag{14}$$

From Eqs. (12) and (14) it follows that

$$m_1 = q_2\frac{\lambda_2}{N_{21}\lambda_1-\lambda_2}+\frac{N_{21}\Delta_1-\Delta_2}{N_{21}\lambda_1-\lambda_2} \tag{15}$$

where

$$N_{21} = \frac{n_2' - n_2}{n_1' - n_1}. \tag{16}$$

Since $\Delta_1 = d\varepsilon_1$, $\Delta_2 = d\varepsilon_2$, $\lambda_1 = b_1 \varepsilon_1$ and $\lambda_2 = b_2 \varepsilon_2$, we can rewrite Eq. (15) in the form

$$m_1 = q_2 \frac{b_2}{N_{21}\varepsilon_{12} b_1 - b_2} + d \frac{N_{21}\varepsilon_{12} - 1}{N_{21}\varepsilon_{12} b_1 - b_2} \tag{17}$$

where

$$\varepsilon_{12} = \frac{\varepsilon_1}{\varepsilon_2} = \frac{1}{\varepsilon_{21}}. \tag{18}$$

The coefficient N_{21} characterizes the objects under study and their surrounding medium. If the object is surrounded by air, N_{21} is slightly higher than unity. On the other hand, the coefficient ε_{12} characterizes the interferometric system. Normally, this quantity is equal to unity (when $\varepsilon(\lambda) = \text{const}$) or is slightly smaller than unity. Consequently, the term $N_{21}\varepsilon_{12}$ may be assumed to be practically equal to unity, and frequently we can calculate the initial interference order m_1 from the formula

$$m_1 \approx q_2 \frac{b_2}{b_1 - b_2}. \tag{19}$$

However, a result obtained from this formula should be taken as the nearest integer. If, for instance, Eq. (19) gives $m_1 = 12.2$ or 11.9, the true initial interference order m_1 is equal to 12.

It is worthwhile to note that Eq. (19) is similar to Eq. (10); but Eq. (10) is an exact formula for the empty interference field, whereas Eq. (19) is an approximation for the interference image of the object under study. This approximation applies to many transparent objects whose mean dispersion $n_F - n_C$ is not higher than 0.03, especially when the object is very thin and surrounded by air medium.

We also have, analogously to Eqs. (11), a family of equations

$$\Delta_1' = t(n_1' - n_1) = m_1 \lambda_1 = m_1 \varepsilon_1 b_1, \tag{20a}$$

$$\Delta_2' = t(n_2' - n_2) = (m_1 + 0.5)\lambda_2 = (m_1 + 0.5)\varepsilon_2 b_2, \tag{20b}$$

$$\Delta_3' = t(n_3' - n_3) = (m_1 + 1)\lambda_3 = (m_1 + 1)\varepsilon_3 b_3, \tag{20c}$$

$$\Delta_4' = t(n_4' - n_4) = (m_1 + 1.5)\lambda_4 = (m_1 + 1.5)\varepsilon_4 b_4, \tag{20d}$$

$$\Delta_5' = t(n_5' - n_5) = (m_1 + 2)\lambda_5 = (m_1 + 5)\varepsilon_5 b_5, \tag{20e}$$

. . . .

. . . .

which express the optical path differences Δ'_1, Δ'_2, Δ'_3, ... between the interfering wavefronts Σ_1 and Σ_2 at the pointer line L_2 for the wavelengths λ_1, λ_2, λ_3, ... (Fig. 3). It is selfevident that λ_1, λ_2, λ_3, ... and related quantities (m_1, b_1, b_2, b_3, ... and ε_1, ε_2, ε_3, ...) are now different from those in Eq. (11). Any combination of two Eqs. (20) gives a formula similar to Eqs. (17) or (19) from which the initial (m_1) or current (m_1+q_2) order can be calculated if m_1 cannot be identified readily by visual observation.

We can distinguish two basic steps in the VAWI–2 procedure that lead to the determination of the desired quantity, which is the optical path difference δ introduced by an object under study to the interference field. Other quantities, like thickness t and/or refractive index n, can be derived from δ.

The first step is the measurement of the interfringe spacings b_1, b_2, b_3, ... for a number of consecutive interference orders $m = m_1+q_2$ and then to plotting the graphs $b(m)$. One graph is made for the empty interference field and the other for the interference image of the object under study. A result of this operation is shown in Fig. 4 where m_1 is assumed to be 10 for the empty interference field

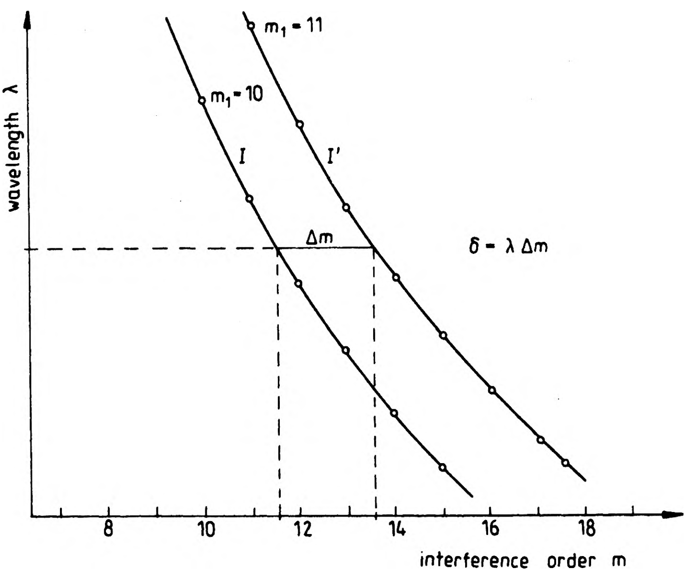

Fig. 4. Determination of the optical path difference δ produced by an object under study

(graph I) and 11 for the object (graph I'). In other words, graphs I and I' express the relative optical path differences Δ/λ and Δ'/λ versus the interfringe spacing b; it is selfevident that $\Delta/\lambda = m$ and $\Delta'/\lambda = m$. Since the interfringe spacing b is strictly defined by the wavelength λ, the graphs I and I' express automatically the optical path differences Δ and Δ' versus the light wavelength λ.

The second step is the determining of the optical path difference δ introduced by the object under study. This operation is simply defined by the relation

$$\delta = \Delta' - \Delta = \lambda\Delta m, \tag{21}$$

where Δm is the difference of the interference orders for any light wavelength as shown in Fig. 4. As can be seen, Δm is the horizontal distance between graphs I and I'.

Note that the first step is performed for the integer interference orders $m = m_1 + q_2$ (high-order interference fringes are brought into coincidence with the pointer line L_2 as shown in Fig. 2**a**), or for the half interference orders (high-order fringes are brought into anticoincidence with the pointer line L_2 as shown in Fig. 2**b**). In the first instance the increment $q_2 = 0, 1, 2, 3, \ldots$, while in the second $q_2 = 0.5, 1.5, 2.5, \ldots$. By contrast, the second step makes it possible to determine the fractional interference orders, e.g., $\Delta m = 0.815, 0.823, 0.832, 0.843, \ldots$ for different, shorter and shorter wavelengths λ. The difference Δm may be an integer number only for some particular situations where δ exceeds the light wavelength λ. In order to determine Δm precisely, the graphs I and I' should be performed in a suitable (large) scale.

The above discussion deals with the transmitted-light VAWI–2 technique, but it also applies to reflected-light interferometry, except that some alterations should be brought into Eqs. (12)–(15), (17) and (20). These alterations result from phase jumps on reflection (see [3]). Fortunately, the same approximative formula (19) can be used for determining the initial interference order m_1. In effect, the same procedure applies to both transmitted-light and reflected-light VAWI–2 techniques.

3. Practical implementation

In general, the reflected-light and transmitted-light VAWI–2 techniques are similar to the original VAWI method. They are especially suitable for the Biolar PI double-refracting microinterferometer described earlier (see Fig. 7 in [1] and Fig. in [3]). One of the most important advantages of this instrument is that it enables the measurement of the wavelength of monochromatic light in real time, as required by the VAWI and VAWI–2 methods, since there exists a rigorous and well defined relation between the interfringe spacing b and the wavelength λ of light entering the interference optical system. The relation between b and λ is nearly linear (see Fig. 8 in [1]), and the graph $b(\lambda)$ is considered as the basic calibration plot.

The Biolar PI microinterferometer is provided with an eyepiece graticule incorporating many parallel lines among which two suitably separated pointer lines L_1 and L_2 (see Figs. 1–3) can be selected and used for the VAWI–2 procedure.

A wedge interference filter is used for continuous variation of the wavelength of light entering the optical system. A halogen lamp (12 V/100 W) is employed as a source of the filtered white light. The local peak wavelengths of the wedge interference filter, i.e., the wavelengths λ_1, λ_2, $\lambda_3, \ldots$ which produce coincidences and/or anticoincidences (see Fig. 2) of high-order fringes with the pointer line L_2, are determined simply by measuring the distances b_1, b_2, $b_3, \ldots$ between interference fringes produced by each of the wavelengths mentioned above. The measurement of these distances is carried out by means of a micrometer screw associated with the transverse movement of the Wollaston prism installed in the interferometric head of the Biolar PI microinterferometer. The prism movement is accompanied with the lateral translation of interference fringes (I and I', Figs. 1 and 2) observed in the image plane. The eyepiece graticule incorporates a central pointer line on which the centres of the interference fringes are guided. It is recommended to measure a multiple interfringe spacing, e.g., the distance between interference fringes of plus and minus ten orders rather than a single interfringe spacing; thus more accurate values of this spacing is obtained. When the interfringe spacings b_1, b_2, b_3, ... are determined, the wavelengths of interest λ_1, λ_2, λ_3, ... are read out from the calibration graph $b(\lambda)$. When one of the particular interfringe spacings b_1, b_2, b_3, ... is measured, the Wollaston prism must be carefully readjusted to its zero position, defined by the coincidence of the pointer line L_1 (see Fig. 1) with the zero-order fringe of the empty interference field.

It is worthwhile to note that the Biolar PI microinterferometer is standardly equipped with a binocular tube; however, a monocular tube is more suitable for very precise visual measurements.

The angle of tilt (ε) of the wavefronts Σ_1 and Σ_2 (see Figs. 1 and 3) produced by a typical Wollaston prism (see [4]) is given by

$$\varepsilon = 2(n_e - n_o)\tan\alpha = 2B\tan\alpha, \tag{22}$$

where α is the apex angle of the prism, $B = n_e - n_o$ is the birefringence, and n_e, n_o are the refractive indices (extraordinary and ordinary) of a material of which the Wollaston prism is made. The coefficient ε_{12} (see Eq. (18)) can now be expressed as

$$\varepsilon_{12} = \frac{B_1}{B_2} = B_{12} \tag{23}$$

and Eq. (17) takes the form

$$m_1 = q_2 \frac{b_2}{N_{21}B_{12}b_1 - b_2} + d\frac{N_{21}B_{12} - 1}{N_{21}B_{12}b_1 - b_2}. \tag{24}$$

This equation applies to the Biolar PI microinterferometer.

Let the difference $\lambda_1 - \lambda_2$ between the light wavelengths be as large as possible within the visible spectrum. We take, for instance, $\lambda_1 = \lambda_C = 656.3$ nm and $\lambda_2 = \lambda_F = 486.1$ nm. The Biolar PI microinterferometer incorporates typical or modified Wollaston prisms made of quartz crystal. Birefringence B_C and B_F of this material is equal to 0.00902 and 0.00929, respectively [5]. Consequently, $B_{12} = 0.00902/0.00929 = 0.971$. On the other hand, the dispersion coefficient N_{FC} of many substances transparent in visible spectrum is equal to 1.02–1.04 (compare Table 1 in [1]). Consequently, the term $N_{21}B_{12}$ in Eq. (24) is equal to 0.99–1.01, and for $N_{21} = 1.03$ the term $N_{21}B_{12} = 0.9991 \approx 1$. We can therefore ignore the second term in Eq. (24) and accept Eq. (19) for determining the initial interference order m_1. Such a situation is very useful for the Biolar PI microinterferometers and other polarization interferometers which use double-refracting elements made of quartz crystal.

Moreover, the Biolar PI microinterferometer produces two laterally sheared images (I'_1 and I'_2) of an object under study. If the object is isotropic, its interference images I'_1 and I'_2 are equivalent but they displace the interference fringes in the opposite direction (compare Figs. 5, 8 and 12). Certainly, both images can be used for measuring the optical path difference δ produced by the object. Returning to Fig. 4, we can construct two graphs I'_1 and I'_2 instead of a single graph I'. The graphs I'_1 and I'_2 will run symmetrically with respect to the graph I which characterizes the empty interference field (compare Figs. 6, 9, 10 and 13). This situation makes it possible to determine the interference order difference $2\Delta m$ instead of Δm. Certainly, the quantity $2\Delta m$ is measured between graphs I'_1 and I'_2 and for the economy of time we can ignore graph I. It is selfevident that Δm will be determined more accurately if we measure the quantity $2\Delta m$. Consequently, more accurate values result from Eq. (21) for the optical path difference δ.

4. Exemplary measurements

In order to illustrate practically the performance of the VAWI–2 method, microinterferometric measurements have been performed on some thin films and layers deposited on glass substrates. As it is a usual case in microinterferometry, the object to be studied should have an edge or a groove on which the displacement of interference fringes is observed. A steep edge is especially required for wavefront shear interferometers, among which there is the Biolar PI microinterferometer described above.

4.1. Vacuum evaporated thin film

Thin film stripes of silicon oxides (SiO_x) were vacuum evaporated on a glass slide through a mask, and the film thickness t was measured then by using the reflected-light VAWI technique described earlier in [3]. The obtained result was $t = 1.8019$ µm. However, the refractive index dispersion $n(\lambda)$ could not be measured effectively by using the transmitted-light VAWI technique since only one fringe coincidence occurred over the visible spectrum for $\lambda_1 = 589$ nm (Fig. 5). This limitation was overcome by using the transmitted-light VAWI–2 technique. The distance d between the pointer lines L_1 and L_2 was selected to be equal to $10b_1$ for $\lambda_1 = 672.5$ nm. The results are listed in Table 1 and explained by graphs in Figs. 6 and 7.

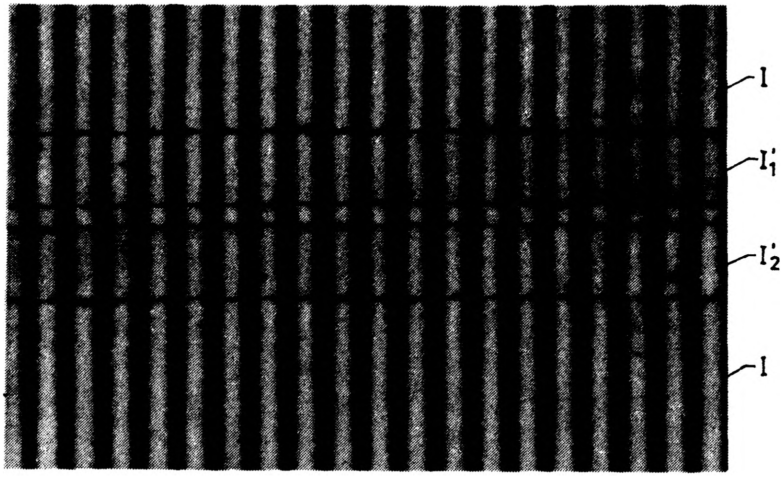

Fig. 5. Microinterferogram of a SiO_x film strip. I – empty interference field (reference fringes), I'_1 and I'_2 – interference fringes displaced by the strip. Print magnification PM = 330 ×

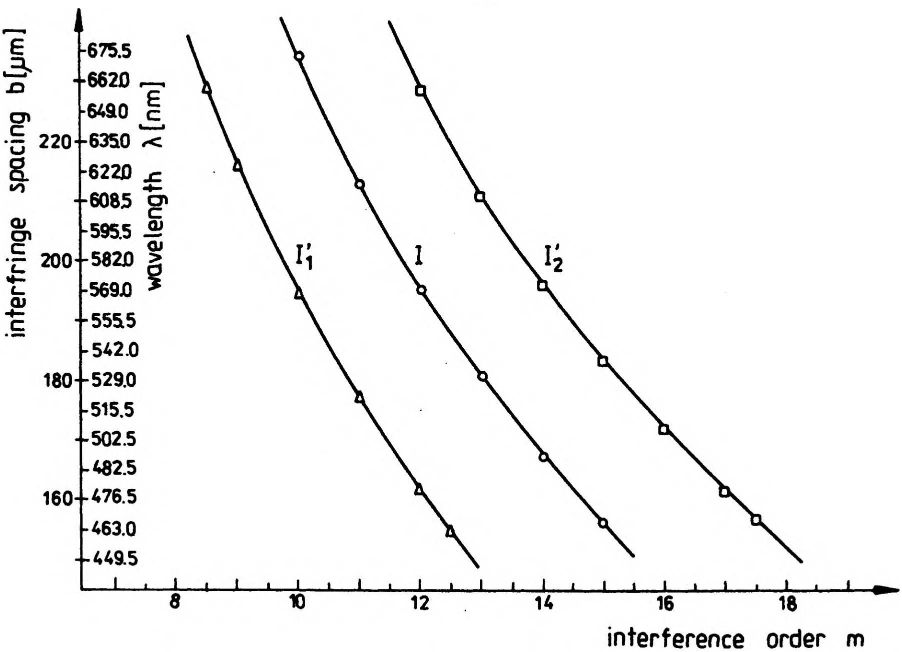

Fig. 6. Transmitted-light VAWI–2 technique; measurement of the refractive index dispersion $n(\lambda)$ of a SiO_x film of thickness $t = 1.8019$ μm. I – graph for empty interference field (see Fig. 5), I'_1 and I'_2 – graphs for the 1st and 2nd interference images of the film strip on which the measurement was performed

Table 1. Results of the measurement of the refractive index dispersion $n(\lambda)$ of a vacuum evaporated SiO_x film of thickness $t = 1.8019$ µm

empty interference field (I, see Figs. 5 and 6)									
q_2	0	1	2	3	4	5			
b [µm]	233.90	212.85	195.34	180.75	167.625	156.50			
initial inteference order $m_1 = 10$									
$m = m_1 + q_2$	10	11	12	13	14	15			
1st interference image of the film strip (I_1, see Figs. 5 and 6)									
q_2	0	−0.5	1	2	3	3.5			
b [µm]	216.025	229.00	194.675	177.25	162.075	154.975			
initial interference order $m_1 = 9$									
$m = m_1 + q_2$	9	8.5	10	11	12	13			
2nd interference image of the film strip (I_2, see Figs. 5 and 6)									
q_2	0	1	2	3	4	5	5.5		
b [µm]	228.625	211.175	196.075	183.70	172.35	161.925	157.55		
initial interference order $m_1 = 12$									
$m = m_1 + q_2$	12	13	14	15	16	17	17.5		
optical path differences δ and refractive indices n for different wavelengths λ									
λ [nm]	463.0	476.5	489.5	502.5	515.5	529.0	542.0	555.5	569.0
δ [µm]	1.2227	1.2074	1.1939	1.1886	1.1861	1.1817	1.1806	1.1714	1.1691
$n = 1 + \delta/t$	1.681	1.670	1.663	1.659	1.658	1.656	1.655	1.650	1.649
λ [nm]	582.0	595.5	608.5	622.0	635.0	649.0	662.0	675.5	
δ [µm]	1.1635	1.1623	1.1582	1.1558	1.1497	1.1463	1.1439	1.1443	
$n = 1 + \delta/t$	1.646	1.644	1.643	1.641	1.638	1.636	1.635	1.635	

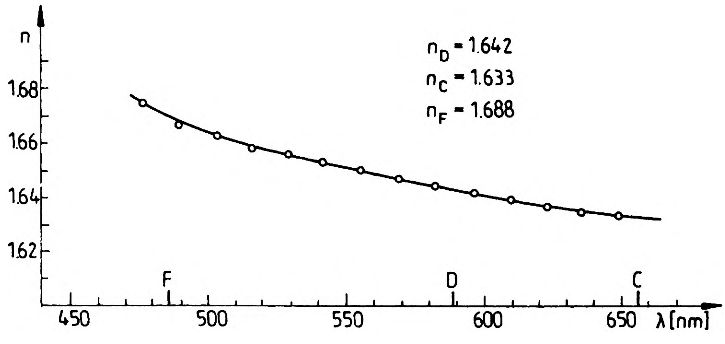

Fig. 7. Result of measurement of the refractive index dispersion $n(\lambda)$ of the SiO film strip shown in Fig. 5

4.2. Photoresist film

A uniform film of photoresist (AZ1350) was standardly deposited on a glass slide and then a groove was made on the film by means of a resor-blade. The interference image of this specimen is shown in Fig. 8. The photoresist film was so thin that its thickness could not be measured by using the reflected-light VAWI technique; no fringe coincidence occurred over the visible spectrum. The reflected-light VAWI–2 technique was therefore used. The pointer lines L_1 and L_2 were separated from each other by the distance $d = 10b_1$ in red light of wavelength $\lambda_1 = 663.0$ nm. The results of measurement are shown in Table 2 and Fig. 9.

The same region of the photoresist film was measured by using the transmitted-light VAWI–2 technique which permitted accurate determination of the refractive index dispersion $n(\lambda)$ of the film. The results are listed in Table 3 and explained by graphs in Figs. 10 and 11.

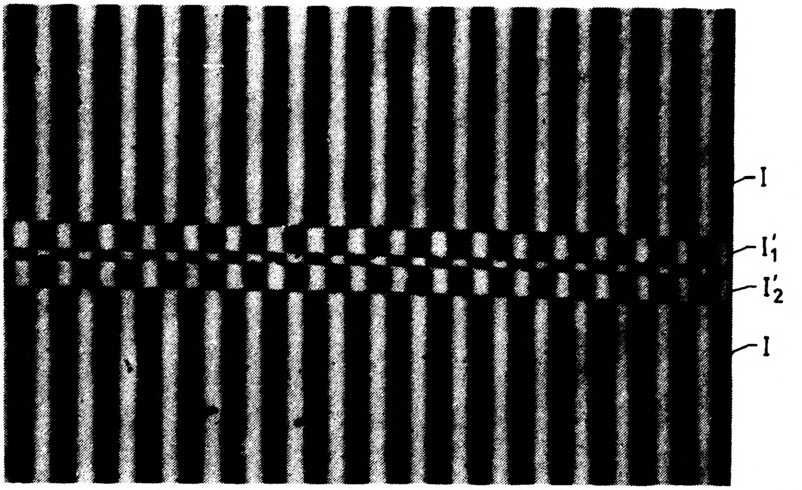

Fig. 8. Microinterferogram of a photoresist film (AZ1350) with a groove penetrating the film down to a glass substrate. I, I'_1, and I'_2 as in Fig. 5 (PM = 170×)

Table 2. Results of the measurement of the thickness (t) of an AZ1350 photoresist film

empty interference field (I, see Figs. 8 and 9)										
q_2	0	1	2	3	4	4.5	5			
b [μm]	116.735	106.05	97.125	88.725	83.325	80.50	77.65			
				initial interference order $m_1 = 10$						
$m = m_1 + q_2$	10	11	12	13	14	14.5	15			
1st interference image of the film (I_1, see Figs. 8 and 9)										
q_2	0	1	2	3						
b [μm]	111.725	100.65	91.55	84.575						
				initial interference order $m_1 = 9$						
$m = m_1 + q_2$	9	10	11	12						
2nd interference image of the film (I_2, see Figs. 8 and 9)										
q_2	0	−0.5	1	2	3	4				
b [μm]	111.25	116.625	102.625	95.075	88.825	83.85				
				initial interference order $m_1 = 12$						
$m = m_1 + q_2$	12	11.5	13	14	15	16				
wavelength λ, optical path difference δ, and thickness t										
λ [nm]	509.0	522.0	535.0	548.5	561.0	574.0	587.5	603.0	613.5	627.0
δ [μm]	0.9416	0.9396	0.9408	0.9324	0.9350	0.9376	0.9400	0.9396	0.9304	0.9300
$t = \delta/2$ [μm]	0.4708	0.4698	0.4704	0.4662	0.4675	0.4688	0.4700	0.4698	0.4652	0.4650
by averaging, $t = 0.4684$ μm										

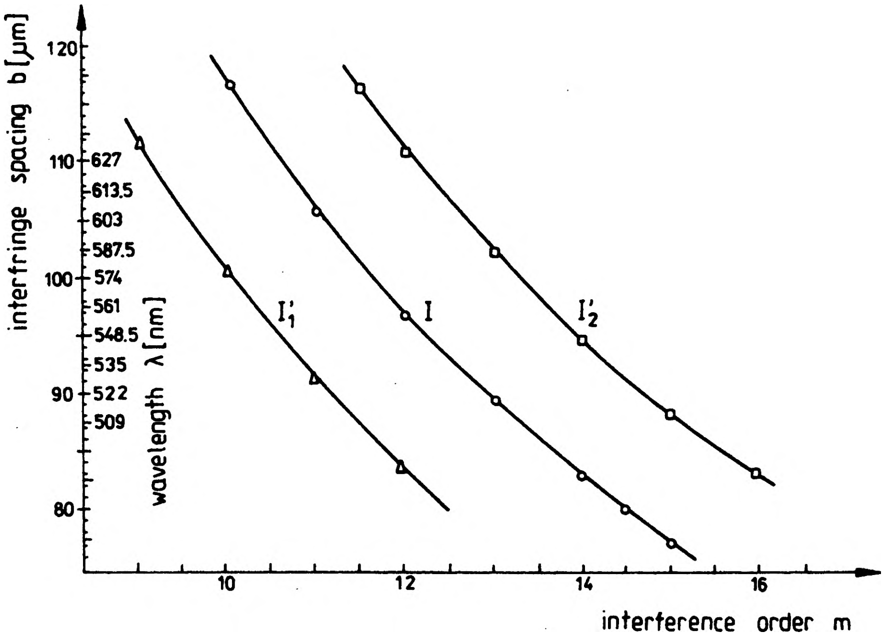

Fig. 9. Reflected-light VAWI–2 technique; thickness measurement of the photoresist film whose interference pattern is shown in Fig. 8. I, I'_1, and I'_2 as in Fig. 6

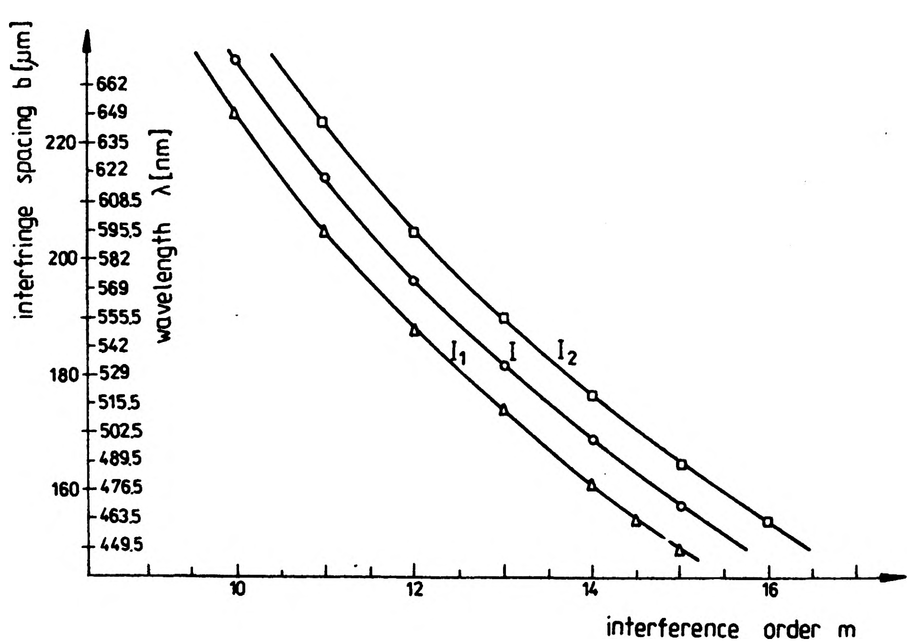

Fig. 10. Transmitted-light VAWI technique; measurement of the refractive index dispersion $n(\lambda)$ of the photoresist film whose interference pattern is shown in Fig. 8. I, I'_1, and I'_2 as in Fig. 6

Table 3. Results of the measurement of the refractive index dispersion $n(\lambda)$ of an AZ1350 photoresist film

empty interference field (I, see Figs. 8 and 10)									
q_2	0	1	2	3	4	5			
b [µm]	234.175	213.575	195.65	181.075	168.525	156.90			
initial interference order $m_1 = 10$									
$m = m_1 + q_2$	10	11	12	13	14	15			
1st interference image of the film (I_1, see Figs. 8 and 10)									
q_2	0	−0.5	1	2	3	4	4.5	5	
b [µm]	225.1	236.025	204.75	188.075	173.925	161.025	154.75	149.725	
initial interference order $m_1 = 10$									
$m = m_1 + q_2$	10	9.5	11	12	13	14	14.5	15	
2nd interference image of the film (I_2, see Figs. 8 and 10)									
q_2	0	−0.5	1	2	3	4	5		
b [µm]	223.525	234.60	204.45	189.725	176.375	164.475	154.725		
initial interference order $m_1 = 11$									
$m = m_1 + q_2$	11	10.5	12	13	14	15	16		
optical path differences δ and refractive indices n for different wavelengths λ									
λ [nm]	449.5	463.0	476.5	489.5	502.5	515.5	529.0	542.0	555.5
δ [µm]	0.7982	0.7925	0.7855	0.7800	0.7785	0.7771	0.7757	0.7743	0.7729
$n = 1 + \delta/t$*	1.704	1.692	1.677	1.666	1.662	1.659	1.656	1.653	1.650
λ [nm]	569.0	582	595.5	608.5	622.0	635.0	649.0	662.0	
δ [µm]	0.3031	0.3012	0.3002	0.2993	0.2984	0.2979	0.2974	0.2974	
$n = 1 + \delta/t$	1.647	1.643	1.641	1.639	1.637	1.636	1.635	1.635	

* $t = 0.4684$ µm (see Table 2)

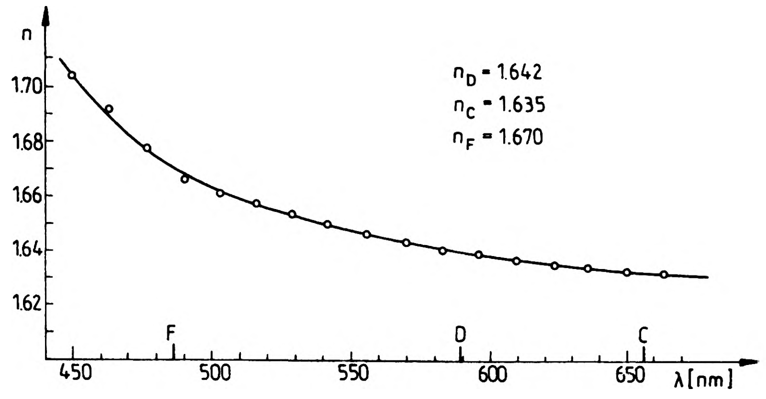

Fig. 11. Result of measurement of the refractive index dispersion $n(\lambda)$ of the AZ1350 photoresist film whose interference pattern is shown in Fig. 8

It is well known that the measurement of the refractive index dispersion $n(\lambda)$ of thin films is a serious problem within the scope of typical interferometric or microinterferometric procedures known to date. This problem is indeed reduced by the VAWI–2 technique used in both transmitted and reflected light.

4.3. Layer of photographic emulsion

This relatively thick layer (Fig. 12) was selected to compare the VAWI and VAWI–2 techniques. The layer thickness t was measured by using only the reflected-light VAWI technique since the VAWI–2 technique was not suitable for this purpose. The result is given in Table 4. The thickness $t = 6.297$ μm refers,

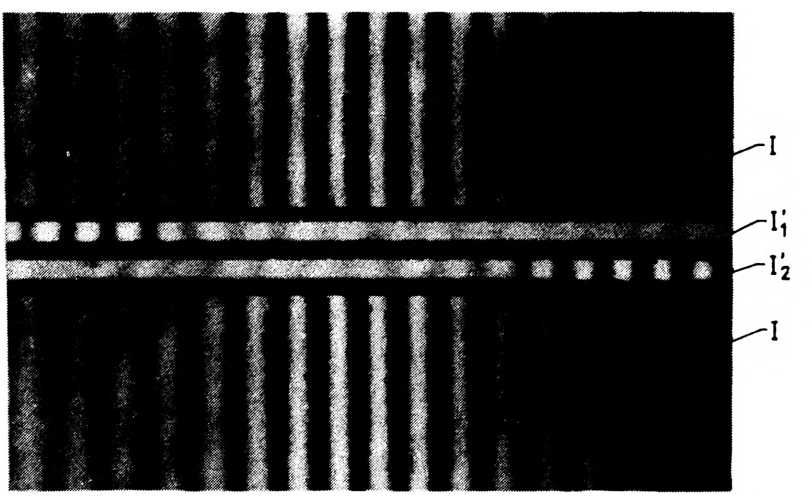

Fig. 12. Microinterferogram (taken in white light) of a Holotest 10E56 emulsion with a groove penetrating the emulsion layer down to the glass substrate. I, I'_1, and I'_2 as in Fig. 5 (PM = 150×)

Table 4. Results of the measurement of the thickness (t) of photosensitive emulsion of a Holotest 10E56 plate (Agfa–Gevaert) by using the reflected-light VAWI technique

q_2	0	1	2	3	4	5
b [μm]	114.825	108.625	102.800	98.150	93.075	88.950
λ [nm]	663.5	630.0	598.5	573.5	547.0	524.5
m_1	–	18.81	18.41	19.12	18.78	18.87
	–	–	18.00	19.30	18.77	18.88
	–	–	–	20.94	19.24	19.26
	–	–	–	–	17.64	18.41
	–	–	–	–	–	19.31
The mean value $\bar{m}_1 = 18.92$, so the initial interference order $m_1 = 19$						
$m = m_1 + q_2$	19	20	21	22	23	24
$\delta = m\lambda$ [μm]	12.6065	12.6000	12.5685	12.6170	12.5810	12.5880
$t = \delta/2$ [μm]	6.3033	6.3000	6.2843	6.3085	6.2905	6.2940
by averaging, $t = 6.297$ μm						

however, to a given region of the specimen since the layer thickness was not uniform over the photographic (holographic) plate (Agfa–Gevaert Holotest 10E56 plate). For instance, the thickness of emulsion was equal to 6.608 μm in other region of the plate.

On the other hand, this specimen was suitable for both techniques in transmitted light. The results of measurement of the optical path difference $\delta = (n-1)t$ and refractive index n are listed in Tables 5 and 6, and graphically compared in Figs. 13–15. As it can be seen, the VAWI and VAWI–2 techniques give the

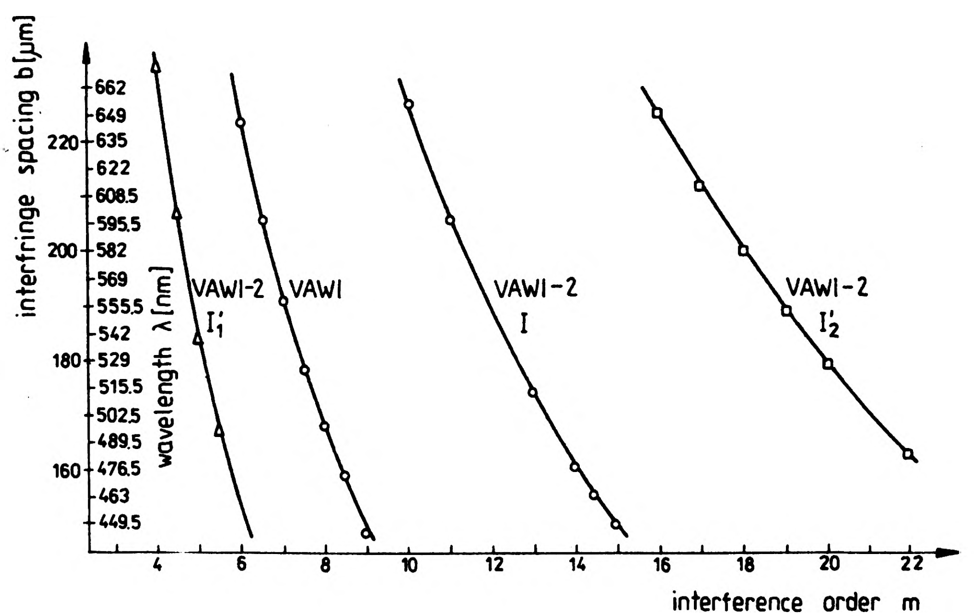

Fig. 13. Transmitted-light VAWI and VAWI–2 techniques applied to the measurement of the refractive index dispersion $n(\lambda)$ of the Holotest 10E56 emulsion whose interference pattern is shown in Fig. 12

Table 5. Results of the measurement of the refractive index dispersion $n(\lambda)$ of the photosensitive emulsion of a Holotest 10E56 plate of thickness $t = 6.297$ (see Table 4) by using the transmitted-light VAWI-2 technique

empty interference field (I, see Figs. 12 and 13)										
q_2	0	1	2	3	4	4.5	5			
b [μm]	231.825	210.90	194.10	179.50	165.950	160.675	155.615			
initial interference order $m_1 = 10$										
$m = m_1 + q_2$	10	11	12	13	14	14.5	15			
1st interference image of the emulsion (I_1, see Figs. 12 and 13)										
q_2	0	0.5	1	1.5	2					
b [μm]	239.433	212.525	189.425	172.40	157.017					
initial interference order $m_1 = 4$										
$m = m_1 + q_2$	4	4.5	5	5.5	6					
2nd interference image of the emulsion (I_2, see Figs. 12 and 13)										
q_2	0	1	2	3	4	5	6			
b [μm]	230.8	217.275	205.50	194.815	185.075	176.80	168.675			
initial interference order $m_1 = 16$										
$m = m_1 + q_2$	16	17	18	19	20	21	22			
optical path differences δ and refractive indices n for different wavelengths λ										
λ [nm]	449.5	476.5	502.5	529.0	555.5	582.0	608.5	635.0	662.0	675.5
δ [μm]	4.1654	4.1297	4.0786	4.0469	4.0274	4.0158	3.9694	3.9434	3.9279	3.9292
$n = 1 + \delta/t$	1.662	1.656	1.648	1.643	1.640	1.638	1.630	1.626	1.624	1.624

Table 6. Results of the measurement of the refractive index dispersion $n(\lambda)$ of the photosensitive emulsion of a Holotest 10E56 plate of thickness $t = 6.297$ (see Table 4) by using the transmitted-light VAWI method

q_2	0	0.5	1	1.5	2	2.5	3
b [μm]	228.77	211.2	196.05	186.68	173.13	162.92	153.83
λ [nm]	659.0	611.5	571.5	538.5	510.5	485.0	460.0
m_1		6.44	6.53	6.70	6.88	6.95	6.93
	The initial interference order cannot be higher than 6, so $m_1 = 6$						
$m = m_1 + q_2$	6	6.5	7	7.5	8	8.5	9
$\delta = m\lambda$ [μm]	3.9540	3.9748	4.0005	4.0388	4.0840	4.1225	4.140
$n \doteq 1 + \delta/t$	1.628	1.631	1.635	1.641	1.649	1.655	1.658

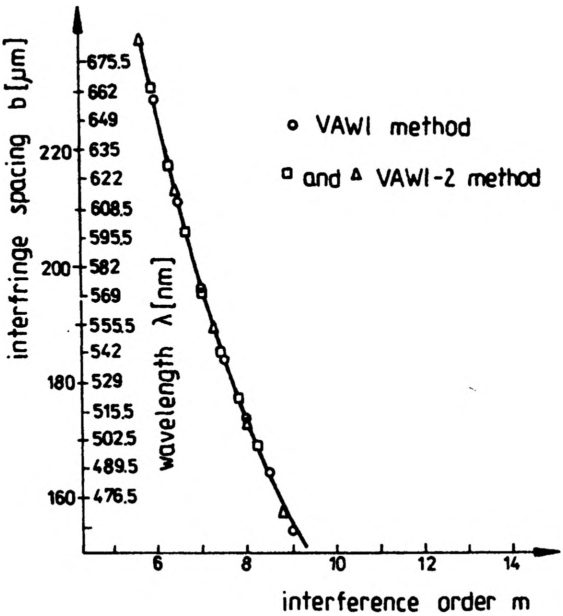

Fig. 14. Result of the optical path difference measurement of the Holotest 10E56 emulsion layer whose interference pattern is shown in Fig. 12; comparison between the VAWI and VAWI–2 techniques operating in transmitted-light

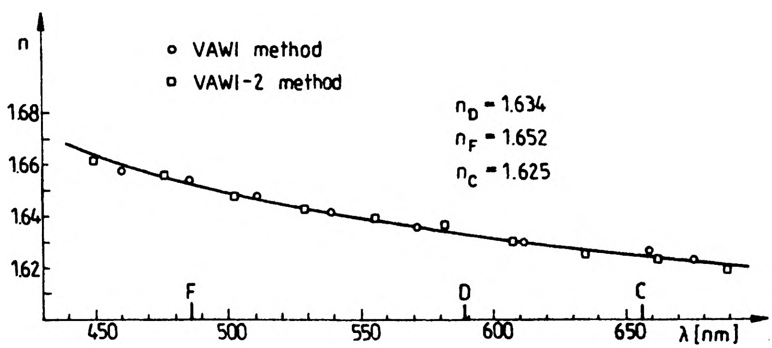

Fig. 15. Refractive index dispersion curve $n(\lambda)$ obtained for the Holotest 10E56 emulsion; comparison between the transmitted-light VAWI and VAWI–2 techniques

same final results for the spectral dispersion of the optical path difference δ and refractive index n. The obtained values for n were additionally confirmed by using the immersion matching method. High-dispersion liquids, available from the Cargille Laboratories (USA), were used to fill a groove in the emulsion layer with immersion medium. The liquid whose refractive index $n_D = 1.635$ at 25° C appeared to be the best matching one. The immersion matching method applied to this kind of optically poor specimens gave the results which agree, within the limit of accuracy, with microinterferometric data presented in Fig. 15.

5. Conclusions

The VAWI–2 method can be treated as a complementary procedure to the original VAWI method described earlier [1, 3]. The transmitted-light and reflected-light VAWI–2 techniques are suitable for measuring relatively thin objects which produce optical path differences (δ) smaller than, say, 3λ. On the other hand, the VAWI techniques function is satisfactorily when the objects to be studied are relatively thick and produce δ higher than, say, 5λ. For intermediate δ, the usefulness of the two methods is alike.

However, the VAWI–2 method is more time-consuming than the VAWI method. After all, both methods require rather a personal computer if they are recommended for routine practice. Nevertheless, the analysis of interference patterns is quite simple and extremely convenient for fully automatic processing.

The VAWI method requires that the reference interference fringes (empty interference field) and the fringes displaced by the object under study be simultaneously present in the field of view of the interferometer as shown in Figs. 5, 8 or 12. This requirement is not necessary if the VAWI–2 method is used; the reference fringes (I) and the fringes (I') displaced by the measured object can be displayed alternatively. This advantage of the VAWI–2 method is especially useful for testing birefringent phase-retarding plates, and will be discussed in a separate paper.

Acknowledgments – I wish to thank Mrs B. Mirkowska and Mrs E. Sobolewska for their help in making the photocopies of interferograms. I also thank Mr J. Pawłowski for his help in preparing the drawings.

References

[1] PLUTA M., Optica Applicata **15** (1985), 375–393.
[2] PLUTA M., Optica Applicata **16** (1986), 141–158.
[3] PLUTA M., Optica Applicata **16** (1986), 159–174.
[4] FRANÇON M., MALLICK S., *Polarization Interferometers*, Wiley–Interscience, London–New York–Sydney–Toronto 1971.

[5] Hardy A. C., Perrin F. H., *The Principles of Optics*, McGraw–Hill Book Company, New York–London 1932.

Received September 15, 1986

Интерферометрия с плавно переменной длиной волны. IV. Альтернативный подход к методу полосатого поля

Раньше описанный интерференционный метод основан на плавной измене длины волны монохроматического света и на подборе таких особых длин волны λ_1, λ_2, $\lambda_3, \ldots$ для которых интерференционные полосы сдвинутые исследуемым объектом находятся в совпадении либо в антисовпадении с несдвинутыми (референтными) полосами. В работе применены две индикаторные линии, лежащие в относительно большом расстоянии по сравнению с периодом интерференционных полос. Во время измерения разницы оптического пути нулевая интерференционная полоса пустого интерференционного поля устанавливается на одну индикаторную линию, а потом изменяя длину волны света с λ_1 по λ_2, $\lambda_3 \ldots$ приводит поочерёдно на вторую индикаторную линию интерференционные полосы высоких порядков $m = m_1$ $m_2 = m_1 + 1$. $m = m_1 + 2, \ldots$. Полный интерференционный порядок считается входным и он должен быть по возможности высоким (например 10 или выше). По этой причине представлен в работе метод можно отнести к методам высокого интерференционного порядка с повышенной точностью измерения.